

Fractional-order fast terminal sliding mode control for nanopositioning

Geng Wang* Sumeet S. Aphale**

* *Key Laboratory of Testing Technology for Manufacturing Process of Ministry of Education, Southwest University of Science and Technology, Mianyang, China (e-mail: geng.wang@swust.edu.cn)*

** *Artificial intelligence, Robotics and Mechatronic Systems Group (ARMS), School of Engineering, University of Aberdeen, UK (e-mail: s.aphale@abdn.ac.uk)*

Abstract: A novel fast terminal sliding mode controller is proposed in this work for high-performance trajectory tracking at the nanometer scales. It combines a recursive integer-order non-singular high-order sliding manifold and a fractional-order fast fixed-time reaching law to ensure globally fast convergence, and adopts a time-delay-estimation based disturbance estimator deeming the designed controller robust to parameter uncertainty. The stability of the designed controller is verified through the Lyapunov framework, where the full analyses of convergence region and settling time are also presented. The tracking performance is experimentally verified on a piezo-stack-driven nano-positioning platform.

Copyright © 2023 The Authors. This is an open access article under the CC BY-NC-ND license (<https://creativecommons.org/licenses/by-nc-nd/4.0/>)

Keywords: high-order sliding mode, fractional calculus, fast fixed-time convergence, time delay estimation, nanopositioning

1. INTRODUCTION

In recent years, piezoelectric nanopositioners have been widely used in some micro/nanoscale high-tech systems, such as atomic force microscopy, nanolithography, microinjection systems, due to its good mechanical robustness, good repeatability, high resolution, and simple design. The performance of piezoelectric platforms is further improved With the progress of control technology. The positioning performance is usually limited by inherent hysteresis, creep, lowly-damped resonant mode, and parameter uncertainty. The key disadvantage of these techniques is the inevitable errors in modeling and parameter identification. Therefore, these techniques are often combined with feedback control to provide adequate performance.

Sliding mode control (SMC) is a popular nonlinear control approach that has recently gained much attention due to its effectiveness and robustness to disturbances. See Feng et al. (2020). The core concept of SMC is to make the system state slide on a specially designed manifold to guarantee a predetermined dynamic performance. The traditional linear SMC method can only guarantee the asymptotic stability of the closed-loop system. See Liu et al. (2015). SMC based on nonlinear sliding surface is also known as terminal sliding mode control (TSMC). The finite-time stability of the terminal sliding mode can significantly improve the speed of the nano-positioning system. However, for the TSMC scheme, the convergence time is highly dependent on the initial conditions. In order to solve this problem, people also propose a fixed time method, that is, the settling time of the stable system is fixed and independent of the initial state of the system. See Ning et al. (2017). To date, these advances have not

been applied to nanopositioning systems to explore the performance improvements they can afford.

Fractional calculus has recently become very attractive in several engineering applications. It has also been proved that the fractional integral sliding surface is equivalent to a low-pass filter on the signum function, and thus can eliminate the high-frequency component. See Shirkavand and Pourgholi (2018). Fractional-order (FO) control systems can provide more adjustable degrees of freedom than their integer-order (IO) counterparts. The work of Kang et al. (2020) also shows the advantages of FO controller over IO design. It is worth noting that the fusion of fractional calculus and fixed-time sliding mode control may be an effective way to improve the performance of some engineering systems. However, to the best of the authors' knowledge, there are no reports on the application of fractional-order fixed-time sliding mode control to piezoelectric actuated high-precision positioning systems. Since fixed convergence time is more attractive than finite time in practice, the fractional calculus-based fixed-time sliding mode control method is still a difficult problem to be explored in piezo-driven positioning systems, which is the main motivation of this paper.

The main focus of this paper is to solve the fixed-time high-precision tracking problem of high-order nonlinear systems based on high-order sliding mode and fractional calculus. We propose a robust high-order sliding mode control method based on a recursive high-order sliding manifold, aiming to improve the positioning performance of piezoelectric platforms. The controller combines recursive high-order sliding manifold, fractional fast fixed-time arrival method and time delay estimation (TDE) method. The main contributions of this work are as follows.

- (1) A new practical robust fractional-order terminal sliding mode control method is synthesized by combining a recursive high-order sliding manifold, a modified fractional-order fast fixed-time reaching law and a TDE disturbance estimation methodology.
- (2) The stability of the proposed controller are theoretically proved via Lyapunov theory.
- (3) The excellent performances of the proposed controller in terms of high tracking accuracy, fast convergence, non-singularity, chattering-free have been verified by comparing with 4 benchmark controllers.

2. MODEL OF THE PLATFORM

Before designing the controller, the model of one axis of a piezoelectric platform must be established.

Firstly, the linear dynamics of the platform is modeled as:

$$y^{(n)}(t) + \sum_{k=0}^{n-1} a_k y^{(k)}(t) = \sum_{k=0}^m b_k u^{(k)}(t) \quad (1)$$

where, $u(t)$ is the input voltage with respect to time t ; $y(t)$ is the output displacement; $u^{(k)}(t)$ and $y^{(k)}(t)$ are respectively the k^{th} derivatives; m and n are the orders of the model, and $m < n$; a_k and b_k are the coefficients of the model. In order to acquire the coefficients and orders of the above model, the dynamics is identified in advance. It is worth noting that the order n in (1) is set to 10, which means the controlled platform is a high-order plant.

Secondly, the inherent hysteresis nonlinearity of the piezoelectric platform is modeled by a hysteresis model. Due to the simplicity and feasibility, the Bouc-Wen model in Wang et al. (2012) is adopted and expressed as:

$$\begin{cases} H(t) = du - h \\ \dot{h} = \alpha_1 \dot{u} - \alpha_2 |\dot{u}| h - \alpha_3 \dot{u} |h| \end{cases} \quad (2)$$

where, $H(t)$ is an immeasurable hysteresis output; d is a constant; h is an intermediate variable whose derivative is \dot{h} ; α_1 , α_2 and α_3 are 3 shape-related parameters for the hysteresis loop.

Finally, with all the other uncertainties considered as a lumped disturbance, the full dynamics of the controlled plant is formulated as:

$$y^{(n)}(t) + \sum_{k=0}^{n-1} a_k y^{(k)}(t) + H(t) + \Delta(t) = \sum_{k=0}^m b_k u^{(k)}(t) \quad (3)$$

where, $\Delta(t)$ is the uncertain displacement caused by the lumped disturbance including all the un-modeled dynamics and other disturbances.

3. CONTROLLER SYNTHESIS

In this section, a robust fractional-order fast terminal sliding mode control scheme with fixed-time convergence law is proposed for controlling the above-mentioned platform. The aim of the control is to accurately track a desired trajectory under unknown disturbances. The main

challenge of combining higher-order sliding mode surfaces, fractional order reaching law, and TDE estimation lies in how to synthesize the control system to make full use of their respective advantages to achieve the desired control performance. The block diagram of the control system is shown in Fig. 1. It should be noted that in this work the fractional order term is approximated by the Oustaloup refined filter method. See Xue et al. (2006). And, the notation $D^{-\alpha}$ and D^α respectively indicate the Reimann-Liouville fractional integration and derivative with the interval from t_0 to t .

3.1 Mathematical foundations

Lemma 1: Monje et al. (2010). Fractional-order differentiation is linear; if A, B are constants, then

$${}_0D_t^\alpha [Af(t) + Bg(t)] = A{}_0D_t^\alpha f(t) + B{}_0D_t^\alpha g(t) \quad (4)$$

$${}_0D_t^\alpha [-f(t)] = -{}_0D_t^\alpha f(t) \quad (5)$$

Lemma 2: Kilbas et al. (2006). For $\mu > 0, v > 0$, the FO calculus of function $f(t) = (t-a)^v$ is

$${}_aD_t^{-\mu} f(t) = \frac{(t-a)^{v+\mu}}{\Gamma(\mu)} B(\mu, v+1) \quad (6)$$

where $B(\mu, v)$ is the beta function, and $\Gamma(\mu)$ is the gamma function.

3.2 Inverse model of hysteresis

In the hysteresis compensation scheme, the inverse hysteresis based on Bouc-Wen model is employed, which is similar to the method proposed in the work of Rakotondrabe (2010). The main idea is that the hysteresis compensation scheme in series of inverse model and Bouc-Wen model can linearize the hysteresis nonlinearity of the system. The specific process is as follows. (i) The Bouc-Wen hysteresis model is identified by a differential evolution algorithm to get the corresponding parameters in formula (2). See Wang et al. (2015). (ii) The output of the inverse hysteresis model can be designed as $\frac{1}{d}(u+h)$. As this is a very mature scheme, interested readers can consult the work of Rakotondrabe (2010) for more details.

3.3 TDE disturbance estimation

After the hysteresis compensation, the full dynamical model is approximated by:

$$y^{(n)}(t) + \sum_{k=0}^{n-1} a_k y^{(k)}(t) + \Delta(t) = \sum_{k=0}^m b_k u^{(k)}(t) \quad (7)$$

As the term $\Delta(t)$ is complicated and can not be easily obtained, in this work it is estimated with the time-delayed method. See Wang et al. (2020). The estimation value of disturbance $\hat{\Delta}(t)$ can be defined as follows:

$$\begin{aligned} \hat{\Delta}(t) \triangleq \Delta(t-T) &= \sum_{k=0}^m b_k u^{(k)}(t-T) - y^{(n)}(t-T) \\ &- \sum_{k=0}^{n-1} a_k y^{(k)}(t-T) \end{aligned} \quad (8)$$

where, T is the sampling interval and then (7) becomes:

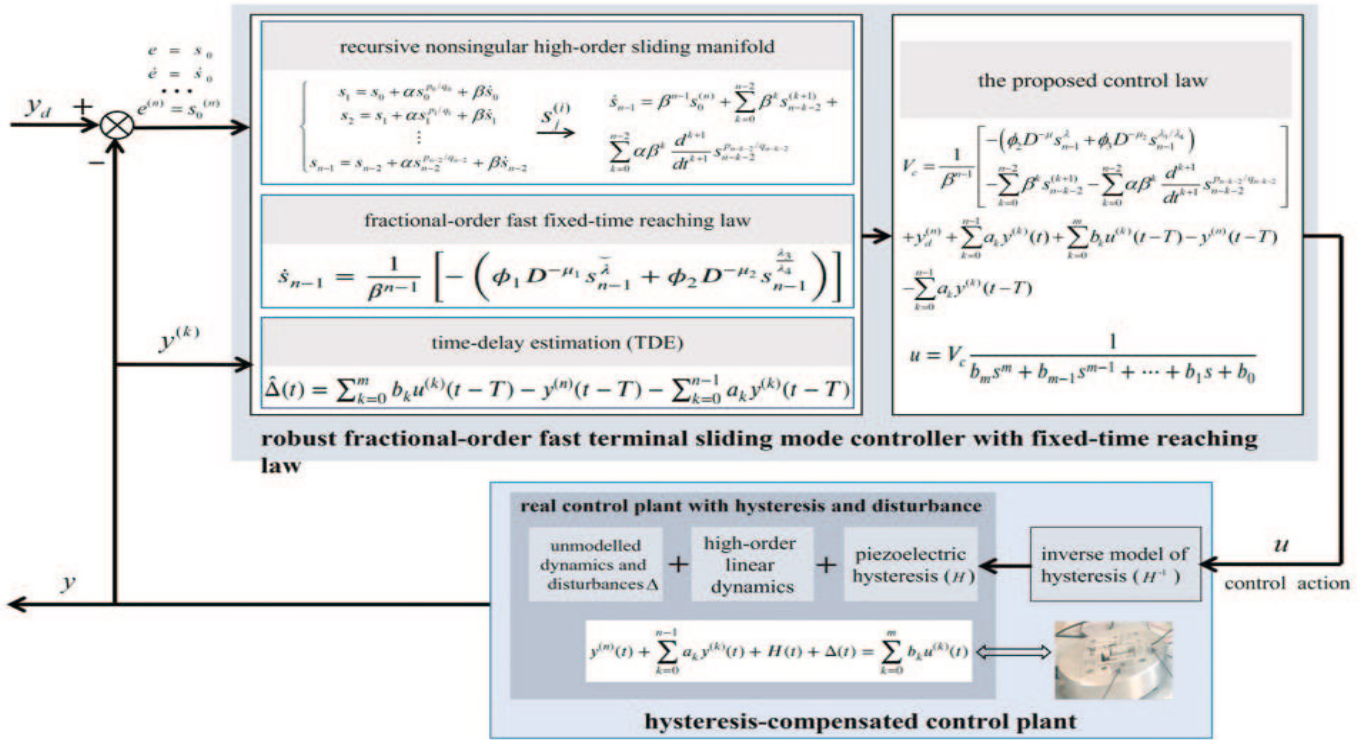


Fig. 1. The proposed overall control scheme

$$y^{(n)}(t) + \sum_{k=0}^{n-1} a_k y^{(k)}(t) + \hat{\Delta}(t) + \tilde{\Delta}(t) = \sum_{k=0}^m b_k u^{(k)}(t) \quad (9)$$

where, $\tilde{\Delta}(t)$ is the estimation error which is defined as:

$$\tilde{\Delta}(t) = \Delta(t) - \hat{\Delta}(t) \quad (10)$$

Usually, according to the characteristics of the actual piezoelectric motion system, we can suppose the estimation error $\tilde{\Delta}(t)$ is bounded and its upper bound is $\bar{\Delta}$.

3.4 Sliding mode based controller design

The control design begins with the design of a recursive high-order sliding manifold which is then followed by a new fractional-order fast fixed-time reaching law.

Define position tracking error:

$$e = y - y_d \quad (11)$$

where y is the real output, and y_d is the command.

Then, we have all the derivatives of the tracking error

$$e^{(i)} = y^{(i)} - y_d^{(i)}, (i = 1, 2, \dots, n) \quad (12)$$

Let

$$s_0 = e, \quad \dot{s}_0 = \dot{e}, \quad \dots, \quad s_0^{(n)} = e^{(n)} \quad (13)$$

A recursive high-order fast terminal sliding manifold is defined as follows:

$$\begin{cases} s_1 = s_0 + \alpha s_0^{p_0/q_0} + \beta \dot{s}_0 \\ s_2 = s_1 + \alpha s_1^{p_1/q_1} + \beta \dot{s}_1 \\ s_3 = s_2 + \alpha s_2^{p_2/q_2} + \beta \dot{s}_2 \\ \vdots \\ s_j = s_{j-1} + \alpha s_{j-1}^{p_{j-1}/q_{j-1}} + \beta \dot{s}_{j-1} \\ s_{n-1} = s_{n-2} + \alpha s_{n-2}^{p_{n-2}/q_{n-2}} + \beta \dot{s}_{n-2} \end{cases} \quad (14)$$

where $\alpha, \beta \in \mathbb{R}^+$; p_j, q_j are all positive and odd, $j = 1, 2, \dots, n-1$; $n-1 < \frac{p_{j-1}}{q_{j-1}} < n$. It should be noted that $n \geq 2$ means $\frac{p_{j-1}}{q_{j-1}} > 1$. This can ensure we don't have zero denominators in the derivation calculations and thus guarantee the non-singularity property. Here, we have the definition: $s^{p/q} \triangleq |s|^{p/q} \text{sign}(s)$. From formula (14) we can get:

$$s_{n-2}^{(2)} = \dot{s}_{n-2} + \alpha \frac{d^2}{dt^2} s_{n-2}^{p_{n-2}/q_{n-2}} + \beta s_{n-2}^{(3)} \quad (15)$$

$$s_{n-3}^{(3)} = \dot{s}_{n-3} + \alpha \frac{d^3}{dt^3} s_{n-3}^{p_{n-3}/q_{n-3}} + \beta s_{n-3}^{(4)} \quad (16)$$

Then, by taking the derivative of the s_{n-1} by recursive steps according to formula (14), we can get:

$$\begin{aligned} \dot{s}_{n-1} &= \dot{s}_{n-2} + \alpha \frac{d}{dt} s_{n-2}^{p_{n-2}/q_{n-2}} + \beta s_{n-2}^{(2)} \\ &= \dot{s}_{n-2} + \beta s_{n-2}^{(2)} + \beta^2 s_{n-2}^{(3)} + \alpha \frac{d}{dt} s_{n-2}^{p_{n-2}/q_{n-2}} \\ &+ \alpha \beta \frac{d^2}{dt^2} s_{n-2}^{p_{n-2}/q_{n-2}} + \alpha \beta^2 \frac{d^3}{dt^3} s_{n-2}^{p_{n-2}/q_{n-2}} + \beta^3 s_{n-2}^{(4)} \\ &= \beta^{n-1} s_0^{(n)} + \sum_{k=0}^{n-2} \beta^k s_{n-k-2}^{(k+1)} + \\ &\sum_{k=0}^{n-2} \alpha \beta^k \frac{d^{k+1}}{dt^{k+1}} s_{n-k-2}^{p_{n-k-2}/q_{n-k-2}} \end{aligned} \quad (17)$$

The following fractional-order fast fixed-time reaching law is proposed due to the satisfactory performance:

$$\dot{s}_{n-1} = \frac{1}{\beta^{n-1}} \left[- \left(\phi_1 D^{-\mu_1} s_{n-1}^{\tilde{\lambda}} + \phi_2 D^{-\mu_2} s_{n-1}^{\frac{\lambda_3}{\lambda_4}} \right) \right] \quad (18)$$

where $D^{-\mu_1}$ and $D^{-\mu_2}$ are the abbreviated forms of ${}_0D_{s_{n-1}}^{-\mu_1}$ and ${}_0D_{s_{n-1}}^{-\mu_2}$, they are the fractional order operators with the orders $0 < \mu_1 < 1$ and $0 < \mu_2 < 1/2$ those are both the ratio of a positive even to a positive odd number and $\tilde{\lambda}$ satisfies the following equation:

$$\tilde{\lambda} = \frac{1}{2} + \frac{\lambda_1}{2\lambda_2} + \left(\frac{\lambda_1}{2\lambda_2} - \frac{1}{2} \right) \text{sign}(|s_{n-1}| - 1) \quad (19)$$

then we have

$$s_{n-1}^{\tilde{\lambda}} = \begin{cases} s_{n-1}^{\lambda_1/\lambda_2} & |s_{n-1}| > 1 \\ s_{n-1} & |s_{n-1}| < 1 \end{cases} \quad (20)$$

Note that λ_i ($i = 1, 2, 3, 4$) are all positive and odd numbers, and $\lambda_1/\lambda_2 > 1$, $0 < \lambda_3/\lambda_4 < 1/2$. Obviously, $\tilde{\lambda} \geq 1$.

Then, we define an intermediate variable:

$$V_c = \sum_{k=0}^m b_k u^{(k)}(t) \quad (21)$$

And, the controlled plant (9) can be rewritten as

$$y^{(n)}(t) + \sum_{k=0}^{n-1} a_k y^{(k)}(t) + \hat{\Delta}(t) + \tilde{\Delta}(t) = V(t) \quad (22)$$

Thus, we proposed the following virtual control law:

$$V_c = \frac{1}{\beta^{n-1}} \left[- \left(\phi_2 D^{-\mu} s_{n-1}^{\tilde{\lambda}} + \phi_3 D^{-\mu_2} S_{n-1}^{\lambda_3/\lambda_4} \right) - \sum_{k=0}^{n-2} \beta^k S_{n-k-2}^{(k+1)} + \sum_{k=0}^{n-2} \alpha \beta^k \frac{d^{k+1}}{dt^{k+1}} S_{n-k-2}^{p_{n-k-2}/q_{n-k-2}} \right] + y_d^{(n)} + \sum_{k=0}^{n-1} a_k y^{(k)}(t) + \hat{\Delta}(t) \quad (23)$$

Combing (8) and the above control law (23), we can get a robust virtual control law as follows:

$$V_c = \frac{1}{\beta^{n-1}} \left[- \left(\phi_2 D^{-\mu} S_{n-1}^{\tilde{\lambda}} + \phi_3 D^{-\mu_2} S_{n-1}^{\lambda_3/\lambda_4} \right) - \sum_{k=0}^{n-2} \beta^k S_{n-k-2}^{(k+1)} - \sum_{k=0}^{n-2} \alpha \beta^k \frac{d^{k+1}}{dt^{k+1}} S_{n-k-2}^{p_{n-k-2}/q_{n-k-2}} \right] + y_d^{(n)} + \sum_{k=0}^{n-1} a_k y^{(k)}(t) + \sum_{k=0}^m b_k u^{(k)}(t - T) - y^{(n)}(t - T) - \sum_{k=0}^{n-1} a_k y^{(k)}(t - T) \quad (24)$$

After the virtual control law V_c is got, we can obtain $u(t)$ from (21). Obviously, V_c is filtered by a filter transfer function $\frac{1}{b_m s^m + b_{m-1} s^{m-1} + \dots + b_1 s + b_0}$. Thus, the ultimate real control law $u(t)$ can be yielded by:

$$u = V_c \frac{1}{b_m s^m + b_{m-1} s^{m-1} + \dots + b_1 s + b_0} \quad (25)$$

The proposed control scheme (25) is illustrated in Fig.1.

Theorem For controlled plant (7) with tracking error satisfying expression (11), if sliding manifold is designed as (14), the reaching surface is designed as (18), and the robust control law (25) can make the control system stable. The system states s_{n-1} will convergence from initial state to a small region σ within a fixed settling time T_{reach} .

$$\text{where } \sigma = \left\{ s_{n-1} : |s_{n-1}| \leq \left(\frac{\beta^{n-1} \tilde{\Delta}}{\phi_2 \frac{\Gamma(\lambda_3/\lambda_4 + 1)}{\Gamma(\mu_2 + \lambda_3/\lambda_4 + 1)}} \right)^{\frac{1}{\lambda_3/\lambda_4 + \mu_2}} \right\},$$

and $T_{reach} < \frac{1}{\phi'_1 (\tilde{\lambda} + \mu_1 - 1)} + \frac{1}{\phi'_2 (1 - \lambda_3/\lambda_4 - \mu_2)}$.

Substituting (8) into (22), we can get

$$y^{(n)}(t) + \sum_{k=0}^{n-1} a_k y^{(k)}(t) + \sum_{k=0}^m b_k u^{(k)}(t - T) - y^{(n)}(t - T) - \sum_{k=0}^{n-1} a_k y^{(k)}(t - T) + \tilde{\Delta}(t) = V(t) \quad (26)$$

Then, combing the virtual control law (24) and the above controller plant (26), we can get

$$\frac{1}{\beta^{n-1}} \left[- \left(\phi_1 D^{-\mu_1} S_{n-1}^{\tilde{\lambda}} + \phi_2 D^{-\mu_2} S_{n-1}^{\lambda_3/\lambda_4} \right) - \sum_{k=0}^{n-2} \beta^k S_{n-k-2}^{(k+1)} - \sum_{k=0}^{n-2} \alpha \beta^k \frac{d^{k+1}}{dt^{k+1}} S_{n-k-2}^{p_{n-k-2}/q_{n-k-2}} \right] = y^{(n)}(t) - y_d^{(n)} + \tilde{\Delta}(t) = e^{(n)}(t) + \tilde{\Delta}(t) = s_0^{(n)}(t) + \tilde{\Delta}(t) \quad (27)$$

From (17), we have

$$s_0^{(n)} = \frac{1}{\beta^{n-1}} \left[\dot{s}_{n-1} - \sum_{k=0}^{n-2} \beta^k s_{n-k-2}^{(k+1)} - \sum_{k=0}^{n-2} \alpha \beta^k \frac{d^{k+1}}{dt^{k+1}} s_{n-k-2}^{p_{n-k-2}/q_{n-k-2}} \right] \quad (28)$$

Substituting formula (28) into formula (27), we get

$$\dot{s}_{n-1} = - \left(\phi_1 D^{-\mu_1} s_{n-1}^{\tilde{\lambda}} + \phi_2 D^{-\mu_2} s_{n-1}^{\lambda_3/\lambda_4} \right) - \beta^{n-1} \tilde{\Delta} \quad (29)$$

A Lyapunov candidate $V = |s_{n-1}|$ is selected and then

$$\begin{aligned} \dot{V} &= \dot{s}_{n-1} \text{sign}(s_{n-1}) \\ &= \left[- \left(\phi_1 D^{-\mu_1} s_{n-1}^{\tilde{\lambda}} + \phi_2 D^{-\mu_2} s_{n-1}^{\lambda_3/\lambda_4} \right) - \beta^{n-1} \tilde{\Delta} \right] \text{sign}(s_{n-1}) \end{aligned} \quad (30)$$

Obviously, when $s_{n-1} > 0$ we can get

$$\begin{aligned} \dot{V} &= -\phi_1 D^{-\mu_1} s_{n-1}^{\tilde{\lambda}} - \phi_2 D^{-\mu_2} s_{n-1}^{\lambda_3/\lambda_4} - \beta^{n-1} \tilde{\Delta} \\ &= -\phi_1 D^{-\mu_1} |s_{n-1}|^{\tilde{\lambda}} - \phi_2 D^{-\mu_2} |s_{n-1}|^{\lambda_3/\lambda_4} - \beta^{n-1} \tilde{\Delta} \end{aligned} \quad (31)$$

When $s_{n-1} < 0$, we can get according to **Lemma 1**:

$$\dot{V} = -\phi_1 D^{-\mu_1} |s_{n-1}|^{\tilde{\lambda}} - \phi_2 D^{-\mu_2} |s_{n-1}|^{\lambda_3/\lambda_4} + \beta^{n-1} \tilde{\Delta} \quad (32)$$

In addition, as $\pm\beta^{n-1}\tilde{\Delta} < \beta^{n-1}\bar{\Delta}$, we can get

$$\dot{V} < -\phi_1 D^{-\mu_1} |s_{n-1}|^{\tilde{\lambda}} - \phi_2 D^{-\mu_2} |s_{n-1}|^{\lambda_3/\lambda_4} + \beta^{n-1}\bar{\Delta} \quad (33)$$

According to **Lemma 2**, we have

$${}_0D_{|s_{n-1}|}^{-\mu_1} |s_{n-1}|^{\tilde{\lambda}} = \frac{B(\mu_1, \tilde{\lambda} + 1)}{\Gamma(\mu_1)} |s_{n-1}|^{\tilde{\lambda} + \mu_1} \quad (34)$$

$${}_0D_{|s_{n-1}|}^{-\mu_2} |s_{n-1}|^{\lambda_3/\lambda_4} = \frac{B(\mu_2, \lambda_3/\lambda_4 + 1)}{\Gamma(\mu_2)} |s_{n-1}|^{\lambda_3/\lambda_4 + \mu_2} \quad (35)$$

For simplicity, ${}_0D_{|s_{n-1}|}^{-\mu_1} |s_{n-1}|^{\tilde{\lambda}}$ and ${}_0D_{|s_{n-1}|}^{-\mu_2} |s_{n-1}|^{\lambda_3/\lambda_4}$ will be abbreviated as $D^{-\mu_1} |s_{n-1}|^{\tilde{\lambda}}$ and $D^{-\mu_2} |s_{n-1}|^{\lambda_3/\lambda_4}$ respectively. Then, according to the expression of beta function, equations (34) and (35) can be re-written as

$$D^{-\mu_1} |s_{n-1}|^{\tilde{\lambda}} = \frac{\Gamma(\tilde{\lambda} + 1)}{\Gamma(\mu_1 + \tilde{\lambda} + 1)} |s_{n-1}|^{\tilde{\lambda} + \mu_1} \quad (36)$$

$$D^{-\mu_2} |s_{n-1}|^{\lambda_3/\lambda_4} = \frac{\Gamma(\lambda_3/\lambda_4 + 1)}{\Gamma(\mu_2 + \lambda_3/\lambda_4 + 1)} |s_{n-1}|^{\lambda_3/\lambda_4 + \mu_2} \quad (37)$$

Note that the value of gamma function is positive because the parameters meet the conditions $\tilde{\lambda} \geq 1$, $0 < \lambda_3/\lambda_4 < 1/2$, $0 < \mu_1 < 1$, $0 < \mu_2 < 1/2$.

Substituting (36) and (37) into (33), we can have

$$\begin{aligned} \dot{V} < & -\phi_1 \frac{\Gamma(\tilde{\lambda} + 1)}{\Gamma(\mu_1 + \tilde{\lambda} + 1)} |s_{n-1}|^{\tilde{\lambda} + \mu_1} \\ & -\phi_2 \frac{\Gamma(\lambda_3/\lambda_4 + 1)}{\Gamma(\mu_2 + \lambda_3/\lambda_4 + 1)} |s_{n-1}|^{\lambda_3/\lambda_4 + \mu_2} \\ & + \frac{\beta^{n-1}\bar{\Delta}}{|s_{n-1}|^{\lambda_3/\lambda_4 + \mu_2}} |s_{n-1}|^{\lambda_3/\lambda_4 + \mu_2} \end{aligned} \quad (38)$$

Then we define two new variables ϕ'_1 and ϕ'_2

$$\phi'_1 = \phi_1 \frac{\Gamma(\tilde{\lambda} + 1)}{\Gamma(\mu_1 + \tilde{\lambda} + 1)} \quad (39)$$

$$\phi'_2 = \phi_2 \frac{\Gamma(\lambda_3/\lambda_4 + 1)}{\Gamma(\mu_2 + \lambda_3/\lambda_4 + 1)} - \frac{\beta^{n-1}\bar{\Delta}}{|s_{n-1}|^{\lambda_3/\lambda_4 + \mu_2}} \quad (40)$$

By substituting (39) and (40) into (38), we can get

$$\dot{V} < -\phi'_1 |s_{n-1}|^{\tilde{\lambda} + \mu_1} - \phi'_2 |s_{n-1}|^{\lambda_3/\lambda_4 + \mu_2} \quad (41)$$

Obviously, we can get $\dot{V} < 0$ if $\phi'_1 > 0$ and $\phi'_2 > 0$. In fact, ϕ'_1 is always positive according to (39) and the range of the value of the parameters. In addition, the 1st term in (40) can be a very big positive and the 2nd term is a very

small positive number. Then $\phi'_2 > 0$ holds if appropriate parameters are chosen. Thus, $\dot{V} < 0$ can be obtained. So, the system stability is proved.

4. EXPERIMENTAL RESULTS

To demonstrate the performance benefits furnished by the proposed controller, a battery of comparative experiments were performed and, the results are presented here.

In order to compare the tracking performance, the percent maximum (MAX) and root-mean-squared (RMS) error indicators are employed for quantitative evaluation. Triangular waves of 25 Hz and 50 Hz were chosen in the experiments. The positioning performance of the proposed controller was compared with three suitably designed controllers that have emerged as benchmark schemes over the years. The first control scheme is a common PID type with the transfer function $C_{PID} = 1.5 + \frac{6500}{s} + 0.0005s$ tuned with the high-order model. The second control scheme is a damping and tracking controller. See Moon et al. (2017). The Positive Position Feedback (PPF) damping controller is combined with an integral action and its transfer function is $C_{PPF} = \frac{6.320 \times 10^7}{s^2 + 11740s + 4.855 \times 10^7}$ and the corresponding integral gain $K_I = 1494$. The third control scheme is a fully tuned conventional linear high-order sliding mode control (LSMC) scheme in the work of Levant (2003), employed to achieve a relatively fair contrast and modified with equivalent and switching actions to deal with this high-order plant. The designed sliding mode surface is in the form of $\sum_{i=0}^9 c_i e^{(i)}$, and the switching action is $2s + 0.05\text{sign}(s)$. The comparison of the trajectory tracking performance is shown in Fig. 2. Obviously, the MAX and RMS errors of the proposed controller are significantly reduced compared with PPF+I, PID, and LSMC controller.

5. CONCLUSIONS

A new robust fractional-order fast terminal sliding model control approach with high-order sliding model dynamics is proposed for a piezoelectric-actuated precision positioning platform. With the well-established accurate model of the controlled plant, the controller is synthesized with the aid of *Inverse model of hysteresis*, *TDE disturbance estimation*, and *Sliding mode based control design*. The recursive high-order sliding manifold and fractional-order fast fixed-time reaching law can guarantee a faster response and fixed convergence time while avoiding potential singularity and chattering problems. The stability of the proposed scheme has been proved via the Lyapunov framework. The excellent performances of the proposed controller have been verified in terms of high tracking accuracy, fast convergence, non-singularity.

REFERENCES

- Feng, Z., Liang, W., Ling, J., Xiao, X., Tan, K.K., and Lee, T.H. (2020). Integral terminal sliding-mode-based adaptive integral backstepping control for precision motion of a piezoelectric ultrasonic motor. *Mechanical System and Signal Processing*, 144, 106856.

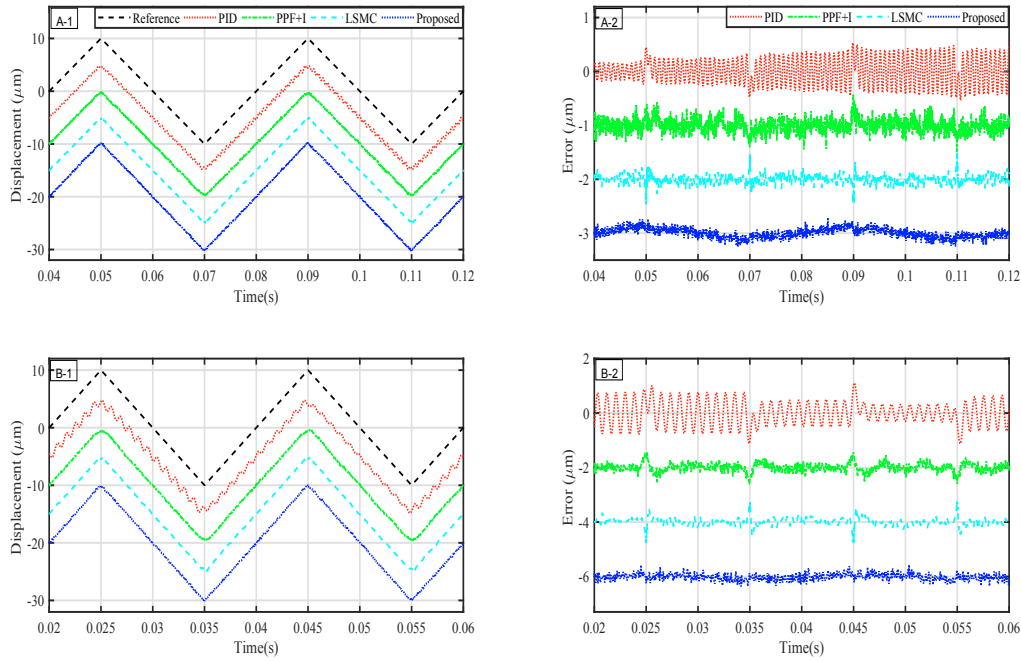


Fig. 2. Closed-loop performance for tracking 25 Hz and 50 Hz triangular references (A-1, B-1). The errors are shown in (A-2, B-2). These plots are offset adequately to show clearly.

- Kang, S., Wu, H., Yang, X., Li, Y., and Wang, Y. (2020). Fractional-order robust model reference adaptive control of piezo-actuated active vibration isolation systems using output feedback and multi-objective optimization algorithm. *Journal of Vibration and Control*, 26(1-2), 19–35.
- Kilbas, Anatoliĭ, A., Srivastava, H.M., and Trujillo, J.J. (2006). *Theory and applications of fractional differential equations*. Elsevier.
- Levant, A. (2003). Higher-order sliding modes, differentiation and output-feedback control. *International journal of Control*, 76(9-10), 924–941.
- Liu, K., Cao, Y., Wang, S., and Li, Y. (2015). Terminal sliding mode control for landing on asteroids based on double power reaching law. In *2015 IEEE International Conference on Information and Automation*, 2444–2449.
- Monje, C.A., Chen, Y., Vinagre, B.M., Xue, D., and Feliu-Batlle, V. (2010). *Fractional-order systems and controls: fundamentals and applications*. Springer Science & Business Media.
- Moon, R.J., San-Millan, A., Aleyaasin, M., Feliu, V., and Aphale, S.S. (2017). Selection of positive position feedback controllers for damping and precision positioning applications. In *Asian Simulation Conference*, 289–301. Springer.
- Ning, B., Han, Q.L., and Zuo, Z. (2017). Distributed optimization for multiagent systems: An edge-based fixed-time consensus approach. *IEEE transactions on cybernetics*, 49(1), 122–132.
- Rakotondrabe, M. (2010). Bouc–wen modeling and inverse multiplicative structure to compensate hysteresis nonlinearity in piezoelectric actuators. *IEEE Transactions on Automation Science and Engineering*, 8(2), 428–431.
- Shirkavand, M. and Pourgholi, M. (2018). Robust fixed-time synchronization of fractional order chaotic using free chattering nonsingular adaptive fractional sliding mode controller design. *Chaos, Solitons and Fractals*, 113, 135–147.
- Wang, G., Chen, G., and Bai, F. (2015). Modeling and identification of asymmetric bouc–wen hysteresis for piezoelectric actuator via a novel differential evolution algorithm. *Sensors and Actuators A: Physical*, 235, 105–118.
- Wang, Y., Zhu, K., Chen, B., and Jin, M. (2020). Model-free continuous nonsingular fast terminal sliding mode control for cable-driven manipulators. *ISA Transactions*, 98, 483–495.
- Wang, Z., Zhang, Z., and Mao, J. (2012). Precision tracking control of piezoelectric actuator based on bouc–wen hysteresis compensator. *Electronics letters*, 48(23), 1459–1460.
- Xue, D., Zhao, C., and Chen, Y. (2006). A modified approximation method of fractional order system. In *2006 International conference on mechatronics and automation*, 1043–1048. IEEE.